

Capacity-Achieving Probabilistic Constellation Shaping for Unamplified Coherent Links

Beatriz M. Oliveira^(1*), Jorge H. Silva⁽¹⁾, Manuel S. Neves⁽¹⁾, Fernando P. Guiomar⁽¹⁾,
Maria C. R. Medeiros⁽²⁾, Paulo P. Monteiro⁽¹⁾

⁽¹⁾ Instituto de Telecomunicações and University of Aveiro, Campus Universitário de Santiago, 3810-193, Portugal
⁽²⁾ Univ Coimbra, Instituto de Telecomunicações, Department of Electrical and Computer Engineering, 3030-290, Portugal
*beatriz.oliveira@av.it.pt

Abstract In unamplified coherent systems, the conventional use of Maxwell-Boltzmann (MB) in probabilistic constellation shaping is largely sub-optimal. We optimize the probability mass function for these systems, and experimentally show a link budget gain of 4.1 dB at 400 Gbps. ©2023 The Author(s)

Introduction

With short-reach links requiring higher data rates and imposing increasingly stringent requirements to the currently deployed intensity modulation and direct detection (IM-DD) schemes, coherent short-reach systems emerge as a way of meeting these requirements. In order to achieve a cost and power efficient short-reach link, all of the optical amplification can be removed, giving rise to the recently standardized use of unamplified coherent systems^[1]. However, unamplified links have inherently different characteristics from the typically deployed amplified links. This is because the main limiting factor for unamplified links is now the peak power, as opposed to the average power, which is described as a peak power constraint (PPC)^[2]. In PPC channels, the peak-to-average power ratio becomes particularly relevant, and advanced modulation formats that have proved to be well-suited for amplified systems require further analysis.

Probabilistic constellation shaping (PCS) based on a Maxwell-Boltzmann (MB) distribution is being used in amplified links to achieve data rate flexibility and increased performance^[3]. However, by attributing higher probability to low-amplitude symbols, the PAPR of the signal significantly increases. The use of MB-based PCS in unamplified systems is then put at question^[2], since it requires extensive tailoring to be beneficial^[4]. Therefore, in order to enable PCS in unamplified systems, other probability mass functions (PMF) should be implemented. A particularly interesting PMF is the reverse MB distribution, in which the outer symbols have higher probabilities^[5]. This leads to a PAPR reduction, and enabled an off-the-shelf use of PCS in an unamplified coherent system with low-order constellations in our previous work^[6]. Nevertheless, the reverse MB might not be the optimum solution for unamplified systems, and optimization of the PMF under a peak power constraint becomes necessary. Previous optimization of the distribution for PCS has been reported for both amplified^[7], and unamplified IM-DD systems^{[8],[9]}. However, PCS optimization for

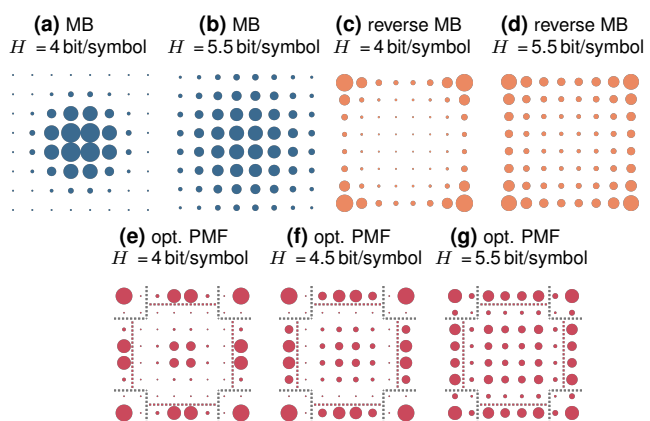


Fig. 1: Generated constellations for each probability mass function, at entropies of a),c),e) $H = 4$ bit/symbol, b),d),g) $H = 5.5$ bit/symbol, and f) $H = 4.5$ bit/symbol.

coherent unamplified systems is still missing.

In this work, we implement a Blahut-Arimoto (BA) method^[10] to optimize the PMF for unamplified systems. We show the yielded constellations and PAPR for the optimized solution, the MB and reverse MB distributions. We experimentally assess the performance for each PMF, for a constellation size of 64 symbols, and for bit rates ranging from 260 Gbps to 600 Gbps.

Defining the Probability Mass Functions

In this work, we implement three probability mass functions (PMFs): the well-known Maxwell-Boltzmann (MB) distribution, as given by (4) in the PCS seminal work^[3], the reverse MB (rMB) distribution, in which a symmetric exponential argument is used instead^[5], and an optimized distribution for unamplified systems using the Blahut-Arimoto (BA) method^[10].

For the BA-generated constellations, we conducted an offline optimization in a peak-power constrained (PPC) additive white Gaussian noise (AWGN) channel. We selected noise power values so that the resulting entropies belong to the range $H = [2, \log_2(M)]$ bit/symbol, and yielding a maximum step of 0.1 bit/symbol, where $M = 64$ is the constellation size.

Figure 1 shows the generated probability mass functions for MB, reverse MB and BA-optimized PCS at entropies of $H = \{4, 4.5, 5.5\}$ bit/symbol. For the optimized constellations, we can observe

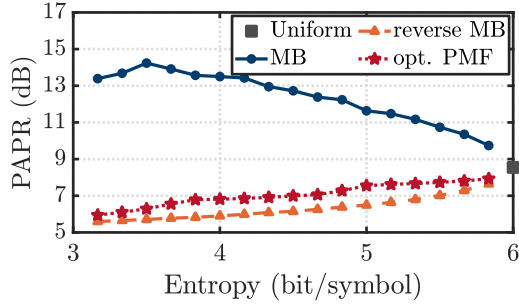


Fig. 2: Peak-to-average power ratio (PAPR) for each entropy. three different behaviors that can be sorted into three groups, depicted in Figs.1e–1g: i) Tier-I, composed of the four symbols constituting the outer-QPSK constellation symbols, and the immediately adjacent symbols, ii) Tier-II, composed of the surrounding outer-square symbols, from which we exclude the previous points, and iii) Tier-III, composed of the remaining constellation symbols. For all entropy values, the symbols in Tier-I follow a reverse MB-like distribution, thus being the main contributors to the reduction of the peak-to-average power ratio (PAPR). At low entropy values (i.e., high noise power), the symbols in Tier-II follow a Gaussian-like probability distribution to account for the high noise. As the entropy increases (i.e., the noise power reduces), these symbols approach a similar distribution found in the reverse MB constellations, since the quality of the channel has now increased and the PPC is playing a more significant role. Similarly, the symbols in Tier-III start by following a Gaussian-like distribution, and then approach the reverse MB distribution. Despite having similar behaviors, we can see a clear break between the symbols in Tier-II and Tier-III, which is highlighted at low entropies with the zero-probability symbols surrounding these zones. In fact, this is a particularly interesting aspect of the optimized solution: contrary to amplified systems, in which a continuous PMF is required (i.e., the non-zero-probability symbols are grouped), a discontinuous PMF is instead beneficial for unamplified systems.

Peak-to-Average Power Ratio

Due to the particular relevance of the peak power in unamplified systems, we start our analysis by showing the achieved peak-to-average power ratio (PAPR) for each probability mass function and constellation entropy in Fig. 2, where the PAPR of the uniform constellation is also shown as a benchmark. We assume a 60 Gbaud signal and a root-raised cosine pulse shaping with a roll-off of $\alpha = 0.2$. The PAPR is collected using Monte-Carlo simulations with 10^3 independent realizations of different transmitted data patterns of length 2^{17} . The MB-distribution yields the highest PAPR of among all PMFs, since the majority of the symbols are located at low amplitudes. As the bit rate increases, the occurrence of high amplitude symbols increases, and the PAPR decreases from 13.4 dB at $H = 3.2$ bit/symbol to 9.7 dB at

$H = 5.8$ bit/symbol. In contrast with the MB distribution, it is worth noting that both the reverse MB and the BA-optimized PMF show a trend of decreasing PAPR as more shaping is applied, achieving a PAPR roughly in the range of 5.5 dB at the lowest tested entropy. This clearly highlights the fact that these distributions are better tailored to unamplified links, where the PAPR ultimately governs the system performance. Interestingly, we observe that the reverse MB actually yields the lowest PAPR (a gap of ~ 0.3 dB w.r.t. the BA-optimized solution) across all tested entropies, which underpins the motivation for its heuristic use in many recent works^{[2],[5],[6]}.

Experimental Setup

Figure 3a shows a diagram of the experimental setup. At the transmitter side, the numerically optimized constellations are loaded for each entropy, while using similar baudrate (60 Gbaud) and pulse shaping ($\alpha = 0.2$). The arbitrary waveform generator (AWG) operating at 120 Gsa/s and ~ 45 GHz bandwidth sends the electrical signal to the radio-frequency (RF) drivers with 23 dB gain to feed the dual-polarization IQ modulator (DP-IQM) that has 35 GHz bandwidth. A tunable laser source (TLS) operating at 1550.12 nm and with a power of 14 dBm provides the optical carrier to the DP-IQM. The unamplified single-span fiber transmission link is emulated using a variable optical attenuator (VOA), as the launched optical power is low enough to avoid causing nonlinearities from the fiber, and we consider an ideal chromatic dispersion compensation at the receiver. At the receiver-side, another TLS operating at 1550.12 nm and with a power of 14 dBm serves as a local oscillator (LO) for the coherent receiver that has a bandwidth of 40 GHz. Four real-time oscilloscopes (RTOs) with bandwidths of 70 GHz digitize the signal at 200 Gsa/s. The receiver-side digital signal processing (DSP) block applies analog frontend correction (skew compensation, Gram-Schmidt orthonormalization, and DC removal), followed by a constant modulus algorithm (CMA) with 15 taps, frequency and carrier phase recovery, and a 51-tap least-mean squares (LMS) equalizer.

We start by defining the uniform net bit rate as $R_{b,\text{uniform}} = 2R_s \log_2(M)R_{\text{FEC}}$, where $R_s = 60$ Gbaud defines the gross symbol rate, $M = 64$ is the constellation size, $R_{\text{FEC}} = 5/6$ is the forward error correction (FEC) rate, and the factor two accounts for the two polarizations. We then sweep the net bit rate, R_b , starting at $R_{b,\text{uniform}}$ and decreasing with steps of 20 Gbps. For each R_b , we compute the required entropy as $H = \frac{R_b}{2R_s} + (1 - R_{\text{FEC}}) \log_2(M)$. The system performance is first evaluated in terms of normalized generalized mutual information (NGMI), which is used to set the NGMI threshold, $\text{NGMI}_{\text{th}} = R_{\text{FEC}}$, assuming ideal coding^[3]. We realize link loss sweeps from 1 to 25 dB, with 1 dB steps. The link

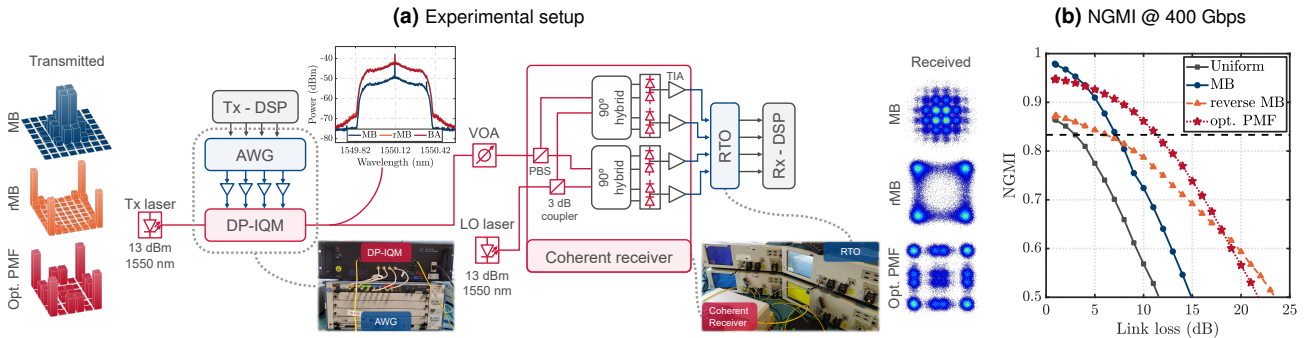


Fig. 3: a) Diagram of the experimental setup, transmitted and received constellations, and the optical spectra after the DP-IQM. b) Experimental performance in terms of NGMI for each PMF at 400 Gbps, and for uniform constellation.

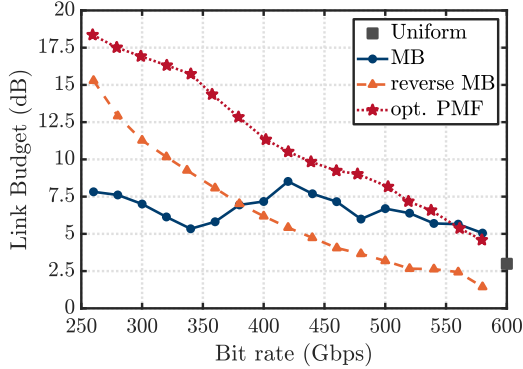


Fig. 4: Experimentally achieved link budget for each PMF and bit rate, and for the uniform constellation. The link budget, defined as the maximum supported link loss at the NGMI threshold, is then evaluated.

Experimental Results

Figure 3b shows the achieved NGMI as a function of link loss, for each PMF at 400 Gbps, while also showing the uniform constellation (600 Gbps) as a benchmark. The NGMI threshold is depicted here with the black dashed horizontal line. Despite achieving the best performance at low link loss, the MB distribution quickly degrades, evidencing the peak-power constraint as the main performance limitation, and crossing the NGMI threshold at a link loss of 7.2 dB. The optimized PMF achieves the highest link budget, crossing the NGMI threshold at 11.3 dB, outperforming the MB distribution by 4.1 dB. Despite yielding the lowest PAPR, the reverse MB distribution is here outperformed by both the MB and optimized PMF distributions, yielding a gap of 1 dB and 5.1 dB, respectively.

By realizing this process for each bit rate, we retrieve the link budget as a function of the bit rate, which is depicted in Fig. 4. The MB distribution achieves a somewhat constant link budget of around 6.5 dB, manifesting the sub-optimal use of this PMF in unamplified systems, since higher shaping (i.e., lower bit rate) is not enabling the performance increase observed in optically amplified systems. The reverse MB distribution is largely outperforming the MB distribution at low bit rates, achieving a gain of 7.4 dB over the MB distribution at 260 Gbps. As the bit rate increases, the performance of the reverse MB distribution decreases and is surpassed by the MB distribution. This is due to the characteristics of the reverse

MB distribution, in which the best performance gains are achieved at higher shaping (lower bit rate), which is a phenomenon that has been reported in previous works^[2]. As expected, the optimized PMF achieves the best performance, outperforming both MB and reverse MB distributions by 10.6 dB and 3.1 dB, respectively, at a bit rate of 260 Gbit/s. The performance gain of the optimized PMF over the reverse MB distribution reaches up to 6.4 dB, at a bit rate of 340 Gbps, and is higher than 3 dB for all bit rates. When compared to the MB distribution, the link budget of the optimized PMF starts by largely surpassing that of the MB distribution, and approaches its performance as the bit rate increases, gradually converging to the uniform solution. Note that, although the BA-optimized constellation should theoretically provide a universal optimum solution, a small gain with the MB distribution is found above 550 Gbps, which can be attributed to a slight mismatch between the ideal unamplified channel considered in the simulations, and the actual experimental system.

Conclusions

As unamplified coherent links become increasingly popular, probabilistic constellation shaping (PCS) that is conventionally implemented using the Maxwell-Boltzmann (MB) distribution is no longer suitable. Using the Blahut-Arimoto method, we optimized the probability mass function (PMF) for these systems. We experimentally assess the performance of the optimized PMF and compare it to both MB and reverse MB distributions. At higher shaping, the performance of the optimized PMF largely surpasses both distributions. The optimized PMF achieves a link budget gain over the reverse MB distribution that exceeds 3 dB for all bit rates. Compared to the MB distribution, the optimized PMF enables a link budget increase around 10 dB for low bit rates, approaching the MB distribution performance as the bit rate increases.

Acknowledgements

This work was partially supported MSCA RISE programme through project DIOR (grant agreement no. 10100828) and by FEDER, through the CENTRO 2020 programme, project ORCIP (CENTRO-01-0145-FEDER-022141), and by FCT/MCTES through project OptWire (PTDC/EEI-TEL/2697/2021) and PhD grants SFRH/BD/143498/2019 and UI/BD/151328/2021. Fernando P. Guiomar acknowledges a fellowship from "la Caixa" Foundation (ID 100010434), code LCF/BQ/PR20/11770015.

References

- [1] OIF, “Unamplified, single wavelength, loss limited link”, *Implementation Agreement 400ZR*, 2020.
- [2] D. Che, J. Cho, and X. Chen, “Does Probabilistic Constellation Shaping Benefit IM-DD Systems Without Optical Amplifiers?”, *Journal of Lightwave Technology*, vol. 39, no. 15, pp. 4997–5007, 2021. DOI: 10.1109/JLT.2021.3083530.
- [3] J. Cho and P. J. Winzer, “Probabilistic Constellation Shaping for Optical Fiber Communications”, *Journal of Lightwave Technology*, 2019.
- [4] B. M. Oliveira, A. Lorences-Riesgo, F. P. Guiomar, M. C. R. Medeiros, and P. P. Monteiro, “Optimizing Probabilistic Constellation Shaping for Amplifier-Less Coherent Optical Links”, *Journal of Lightwave Technology*, vol. 39, no. 13, pp. 4318–4330, 2021. DOI: 10.1109/JLT.2021.3072547.
- [5] M. S. Bin Hossain, G. Böcherer, T. Rahman, *et al.*, “Experimental Comparison of Cap and Cup Probabilistically Shaped PAM for O-Band IM/DD Transmission System”, in *2021 European Conference on Optical Communication (ECOC)*, 2021, pp. 1–4. DOI: 10.1109/ECOC52684.2021.9605995.
- [6] B. M. Oliveira, J. H. Silva, M. S. Neves, F. P. Guiomar, M. C. R. Medeiros, and P. P. Monteiro, “Revisiting Probabilistic Constellation Shaping in Unamplified Coherent Optical Links”, in *Optical Fiber Communication Conference (OFC) 2023*, Optica Publishing Group, 2023, Th3E.1.
- [7] V. Aref and M. Chagnon, “End-to-End Learning of Joint Geometric and Probabilistic Constellation Shaping”, in *Optical Fiber Communication Conference (OFC) 2022*, Optica Publishing Group, 2022, W4I.3. DOI: 10.1364/OFC.2022.W4I.3.
- [8] T. Wiegart, F. Da Ros, M. P. Yankov, F. Steiner, S. Gaiarin, and R. D. Wesel, “Probabilistically Shaped 4-PAM for Short-Reach IM/DD Links With a Peak Power Constraint”, *Journal of Lightwave Technology*, vol. 39, no. 2, pp. 400–405, 2021. DOI: 10.1109/JLT.2020.3029371.
- [9] D. Kim and H. Kim, “Capacity-achieving symbol distributions for directly modulated laser and direct detection systems”, *Opt. Express*, vol. 31, no. 8, pp. 12 609–12 623, Apr. 2023. DOI: 10.1364/OE.484104.
- [10] R. Blahut, “Computation of channel capacity and rate-distortion functions”, *IEEE Transactions on Information Theory*, vol. 18, no. 4, pp. 460–473, 1972. DOI: 10.1109/TIT.1972.1054855.